Structural and Biochemical Exploration of a Critical Amino Acid in Human 8-Oxoguanine Glycosylase[†,‡]

Derek P. G. Norman,[§] Sang J. Chung,[§] and Gregory L. Verdine*

Department of Chemistry and Chemical Biology, Harvard University, 12 Oxford Street, Cambridge, Massachusetts 02138

Received September 9, 2002; Revised Manuscript Received December 10, 2002

ABSTRACT: Members of the HhH-GPD superfamily of DNA glycosylases are responsible for the recognition and removal of damaged nucleobases from DNA. The hallmark of these proteins is a motif comprising a helix−hairpin−helix followed by a Gly/Pro-rich loop and terminating in an invariant, catalytically essential aspartic acid residue. In this study, we have probed the role of this Asp in human 8-oxoguanine DNA glycosylase (hOgg1) by mutating it to Asn (D268N), Glu (D268E), and Gln (D268Q). We show that this aspartate plays a dual role, acting both as an N-terminal α-helix cap and as a critical residue for catalysis of both base excision and DNA strand cleavage by hOgg1. Mutation of this residue to asparagine, another helix-capping residue, preserves stability of the protein while drastically reducing enzymatic activity. A crystal structure of this mutant is the first to reveal the active site nucleophile Lys249 in the presence of lesion-containing DNA; this structure offers a tantalizing suggestion that base excision may occur by cleavage of the glycosidic bond and then attachment of Lys249. Mutation of the aspartic acid to glutamine and glutamic acid destabilizes the protein fold to a significant extent but, surprisingly, preserves catalytic activity. Crystal structures of these mutants complexed with an unreactive abasic site in DNA reveal these residues to adopt a sterically disfavored helix-capping conformation.

The process of aerobic respiration continuously generates reactive oxygen species (ROS)[1] that occasionally escape the mitochondria to cause cellular damage. ROS can also be generated through reaction pathways initiated by ionizing radiation or organic free radicals. ROS are, as a class, ferocious oxidants that react with both cellular proteins and the genome. The principal product of ROS attack on DNA is 8-oxoguanine (*1*, *2*). While guanine pairs in the Watson−Crick sense with cytosine, 8-oxoguanine (oxoG) can form a Hoogsteen pair with adenine during replication, leading to an oxoG·A mispair. Passage of this primary misreplication product through a second round of replication produces a T·A pair, resulting overall in a G·C to T·A transversion mutation; this is the second most common type of somatic mutation found in the p53 gene of human cancers (*3*).

Like most single-base lesions in DNA, oxoG is repaired by the base excision DNA repair pathway (*4*−*7*). The key components of this pathway are lesion-specific DNA glycosylases, enzymes that scan the genome for damaged bases and catalyze scission of their glycosidic bond (Figure 1A). These enzymes fall into two mechanistic classes that employ distinct but related mechanisms. Monofunctional glycosylases use an activated water molecule as the catalytic nucleophile, thereby generating an abasic product via a single transformation. DNA glycosylase/β-lyases use an amine-containing residue on the enzyme as catalytic nucleophile to generate a covalently linked enzyme−DNA adduct, which undergoes a series of subsequent transformations culminating in DNA strand scission on the 3′-side of the lesion. A structural superfamily of these enzymes has been identified (*8*, *9*), the hallmark of which is an active site HhH-GPD motif containing a helix−hairpin−helix (HhH) element (*10*) followed by a Gly/Pro-rich loop and terminating in an invariant Asp residue (Figure 1B). Members of this superfamily are found throughout all three domains of life, Eubacteria, Archaea, and Eukarya, where they serve an essential function in the recognition and removal of a wide variety of damaged DNA lesions, including those resulting from alkylation, oxidation, and hydrolytic deamination, among other forms of genetic insult. The eukaryotic enzyme responsible for repair of oxoG, 8-oxoguanine glycosylase (Ogg1), belongs to the glycosylase/β-lyase mechanistic class of HhH-GPD glycosylases; prototypical monofunctional glycosylases of this superfamily include *Escherichia coli* AlkA and MutY.

[†] This work was supported by NIH Grant GM 51330. D.P.G.N. is supported by an NSF predoctoral fellowship. This work is based upon research conducted at the Cornell High Energy Synchrotron Source (CHESS), which is supported by the National Science Foundation under Award DMR 97-13424, using the Macromolecular Diffraction at CHESS (MacCHESS) facility, which is supported by Award RR-01646 from the National Institutes of Health, through its National Center for Research Resources.

[‡] Coordinates have been deposited with the Protein Data Bank as entries 1N3C, 1N39, and 1N3A for the D268N, D268E, and D268Q hOgg1 structures, respectively.

* Corresponding author. Phone: 617-495-5333. Fax: 617-495-8755. E-mail: verdine@chemistry.harvard.edu.

[§] These authors contributed equally to this work.

[1] Abbreviations: ROS, reactive oxygen species; oxoG, 8-oxoguanine; HhH-GPD, helix−hairpin−helix glycine/proline-rich loop terminated by an aspartic acid; Ogg1, 8-oxoguanine glycosylase; hOgg1, human 8-oxoguanine glycosylase; PAGE, polyacrylamide gel electrophoresis; Tris, 2-amino-2-(hydroxymethyl)-1,3-propanediol; EDTA, ethylenediaminetetraacetic acid; BSA, bovine serum albumin; UDG, uracil DNA glycosylase; UGI, UDG inhibitor; DTT, 1,4-dithiothreitol; CD, circular dichroism; rmsd, root mean square deviation.

10.1021/bi026823d CCC: $25.00
Published on Web 01/24/2003

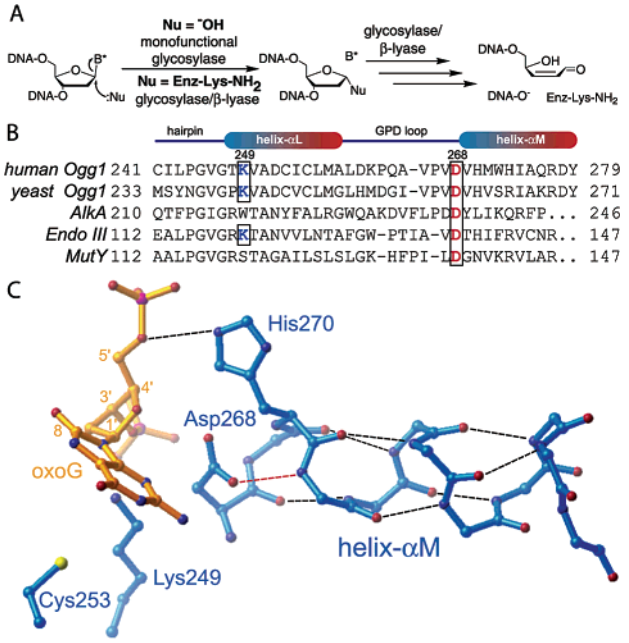

FIGURE 1: (A) Reaction catalyzed by DNA glycosylases. Monofunctional glycosylases use an activated water to displace the lesion base (B*), yielding an abasic product. DNA glycosylase/β-lyases use an internal nucleophilic amino group on the enzyme to displace the lesion base. The initially formed aminal product undergoes ring opening to the corresponding Schiff base (not shown), which then undergoes β-elimination to cleave the DNA backbone on the 3′-side. Hydrolysis then yields the product shown. (B) Sequence and structural alignment of members of the HhH-GPD superfamily. Shown above the aligned sequences is a structural cartoon of all but the N-terminal helix of the HhH-GPD motif, plus the helix that follows the motif. The invariant Asp residue (red, Asp268 in hOgg1) caps the N-terminus of helix α-M. Glycosylase/β-lyases utilize a conserved Lys (Lys249 in hOgg1) as the catalytic nucleophile that displaces the lesion base. (C) Close-up view of the hOgg1 active site, emphasizing the N-capping interaction between the Asp268 side chain and the amide N−H of Met271 (red dashed line) at the N-terminus of helix α-M. This structure was generated by starting from the structure of K249Q hOgg1 bound to oxoG-containing DNA (yellow) (*12*) by modeling in a Lys residue at position 249. No other changes were made. Black dashed lines denote the intrahelical hydrogen-bonding interactions in α-M.

Glycosylase/β-lyases of the HhH-GPD superfamily use an active site Lys positioned within the HhH-GPD motif (Figure 1B; Lys249 in hOgg1) as the catalytic nucleophile. Not surprisingly, this position is occupied by a residue other than Lys in the monofunctional glycosylases (Figure 1B). Notwithstanding the mechanistic distinctions between the two classes of enzymes, both possess a similar overall active site architecture, and both share as the single most highly conserved feature the invariant Asp residue of the HhH-GPD motif (Asp268 in hOgg1; Figure 1B,C). Mutation of the active site Asp residue to Asn severely diminishes or altogether abolishes the catalytic activity of both monofunctional glycosylases (*9*, *11*) and glycosylase/β-lyases (*8*, *10*), thus establishing an essential role for the Asp in catalysis. The precise role of this Asp in catalysis is poorly understood.

Mutation of the catalytic nucleophile in human Ogg1 from Lys to Gln (K249Q hOgg1) generates a form of the protein that forms a stable recognition complex with oxoG-containing DNA (*12*). The crystal structure of K249Q hOgg1 (*12*) complexed with oxoG-containing DNA revealed the overall architecture of the protein/DNA complex and the structural basis for oxoG recognition but shed little light on the function of the active site Asp268. One potential role for Asp268, to deprotonate Lys249 and thereby activate it as a nucleophile, could not be assessed in the original crystal structure because of the K249Q mutation. The crystal structure of wild-type hOgg1 with an abasic inhibitor in DNA demonstrated that, even in the presence of Lys249, Asp268 is sequestered as an end cap for the N-terminus of helix α-M (Figure 1B,C) and is not hydrogen bonded to Lys249 (*13*). These structural findings have raised the alternative possibility that Asp268 does not act as a general base but rather provides electrostatic stabilization for the incipient positive charge that develops on $O^{4'}$ of the substrate during the base excision step. Crystal structures of other members of the HhH-GPD superfamily (*9*, *14*, *15*) invariably show the active site Asp acting as an N-cap for α-M.

In this paper, we study the role of Asp268 in hOgg1 using biochemical and crystallographic analyses. The form of hOgg1 having Asp268 mutated to Asn (D268N hOgg1) is almost completely inactive, though it exhibits stability comparable to that of the wild-type enzyme. The structure of D268N hOgg1 presented here, the first in which both the catalytic Lys and oxoG lesion are present, shows that Asn268 retains its helix-capping interaction with α-M. Mutation of Asp268 to Gln (D268Q hOgg1) and Glu (D268E hOgg1) destabilizes the enzyme thermally, and structural analysis reveals that the mutated residues are present in less favorable helix-capping conformations. Surprisingly, however, both of these mutants are catalytically active.

EXPERIMENTAL PROCEDURES

Expression and Purification of hOgg1 and Its Mutants. A PCR fragment of hOgg1 containing amino acids 12−327 of the human Ogg1 gene was cloned into the pET30a vector (Novagen) using the restriciton sites *Eco*RI and *Hin*dIII. Mutagenesis was performed using the megaprimer mutagenesis method (*16*), and all new constructs were sequenced throughout the hOgg1-coding sequence. Expression and purification of the wild-type and D268N hOgg1 were as described (*12*), but the instability of the D268E and D268Q mutants necessitated modification of the procedure. With the latter two mutant proteins, the induced overexpressing cells were shaken at 16 °C for 24−72 h prior to harvesting. Glycerol (10% v/v) was added to the buffer during all purification, concentration, and storage procedures, which were performed at 4 °C. All forms of hOgg1 showed similar chromatographic behavior on the cation-exchange (Pharmacia Mono-S) and gel-filtration (Pharmacia Sephadex S-200) columns. The enzyme was quantified on the basis of the absorbance at 280 nm, using an extinction coefficient of 37000 cm^{-1} M^{-1}.

Oligonucleotide Synthesis and Labeling. Primers were purchased from Operon (San Diego, CA). The oxoG-containing 25mer oligonucleotide and its complement were synthesized by β-cyanoethyl phosphoramidite solid-phase chemistry on a 1 μmol scale using a commercial oxoG phosphoramidite (Glen Research, Sterling, VA) and were purified by 20% denaturing polyacrylamide gel electrophoresis (PAGE). For crystallization, the oxoG-containing 16mer oligonucleotide and its complement were synthesized and purified similarly. DNA concentrations were determined

using A_{260} quantitation, and radiolabeling reactions were performed with T4 polynucleotide kinase (New England Biolabs, Beverly, MA) and [γ-^{32}P]ATP (10000 Ci/mmol, New England Nuclear).

Single-Turnover DNA-Cleavage Analysis. 5′-^{32}P end-labeled, oxoG-containing duplex DNA (20 nM) was incubated with >500 nM protein in a standard reaction buffer of 50 mM Tris (pH 7.4), 50 mM NaCl, 2 mM EDTA, and 100 μg/mL BSA either at room temperature (D268Q and D268E hOgg1) or 37 °C (D268N hOgg1). Aliquots were removed at various time points and quenched by addition of either 2 volumes of 95% formamide (to observe enzymatic DNA scission) or 2 volumes of 0.5 M piperidine in formamide, followed by heating for 5 min to 60 °C (to observe base removal). The formamide-quenched samples were not heated to avoid spurious thermal DNA strand cleavage of the abasic intermediate. The samples were analyzed on a 20% polyacrylamide gel (8 M urea) in TBE solution (100 mM Tris base, 90 mM boric acid, and 1 mM EDTA) and visualized on a storage phosphorimaging plate (Fuji BAS 1000). Band intensities were quantitated with MacBAS imaging software. Rate constants were determined by fitting the inverse exponential equation to the cleavage data.

For the assays in which abasic DNA was used, 5′-^{32}P end-labeled uracil-containing 25mer duplex DNA was pretreated with uracil DNA glycosylase (UDG, New England Biolabs) for 1 h at 37 °C followed by addition of uracil glycosylase inhibitor (UGI, New England Biolabs). The resulting abasic oligonucleotide was used without further manipulation and could be aliquoted and stored at −20 °C without any detectable decomposition. Radiolabeled abasic DNA (10 nM) was incubated with 2 μM protein, in either the presence or absence of 50 μM 8-aminoguanine in the standard reaction buffer at 8 °C. Aliquots were quenched with formamide and analyzed as above.

Electrophoretic Mobility Shift Assay. Duplex DNA (0.1 nM) was incubated with serial dilutions of protein spanning a concentration from 16 nM to 2.05 μM in 1× binding buffer containing 50 mM Tris (pH 7.4), 100 mM NaCl, 0.5 mM EDTA, 0.5 mM DTT, and 5% glycerol. Protein/DNA binding was allowed to proceed for 20 min at room temperature. The samples were loaded on a prerun 10% nondenaturing polyacrylamide gel (0.5× TBE) and electrophoresed at 200 V for 2 h at room temperature. After drying, the gel was exposed to a storage phosphorimaging plate (Fuji BAS 1000). The proportion of shifted DNA was quantitated with MacBAS imaging software.

Crystallization and X-ray Data Collection. Crystallization was as described for K249Q hOgg1 (*12*). Prior to freezing in liquid nitrogen, crystals were briefly soaked in a solution containing the well solution supplemented with 25% glycerol. X-ray diffraction data (λ = 0.930 Å) were collected at the A1 beamline of CHESS (Cornell) on a CCD detector. Diffraction data were processed using the DENZO/SCALEPACK programming package (*17*).

Model Building and Refinement. Structures were determined by molecular replacement using the structure of K249Q hOgg1 as the initial search model. The CNS programming package (v1.0) (*18*) was used for all refinement. For each mutant, rigid-body refinement was performed, followed by simulated annealing and water placement. Subsequent cycles of $F_o - F_c$ model examination, simulated annealing, and *B*-factor refinement were performed. The conformations of all active site residues were confirmed by simulated annealing omit maps.

Circular Dichroism. Circular dichroism (CD) spectra were recorded on a Jasco J-710 spectropolarimeter in 10 mM potassium phosphate (pH 7.5) and 100 mM KCl in a 0.1 cm cell. The cell temperature was regulated with a Jasco PTC-348W Peltier temperature control. For thermal denaturation experiments, the CD signal was monitored at 222 nm as the temperature was raised from 15 to 70 °C at 1 deg/min. The maximum of the first-derivative plot was taken as the melting point of the protein, except in the case of the D268Q protein, which had no clear maximum in the first derivative. The D268Q hOgg1 melting point was estimated by extrapolation from the temperature scan. See Figure 1 in Supporting Information for the thermal denaturation curves.

RESULTS

Substrate Processing by Wild-Type hOgg1 under Single-Turnover Conditions. Our structural studies on hOgg1, including those presented here, have all employed a truncated version of hOgg1 comprising residues 12−327, the in vitro activity of which is indistinguishable from that of the full-length enzyme (*12*). We have employed this same form in all of the biochemical studies presented here and will refer to it henceforth as hOgg1.

Our first aim was to gain some insight into whether the observed rate of strand scission under pseudo-first-order conditions (large excess of enzyme over substrate) was limited by a chemical transformation or by a conformational change preceding the chemistry. This is an important issue for DNA glycosylases, because these enzymes must recognize a drastically remodeled DNA duplex as a prerequisite to catalysis. These enzymes are also notorious for their slow dissociation from the product of the reaction in vitro, which can obscure kinetic analysis of the initiation phase of the repair reaction. We therefore resorted to single-turnover analysis under pseudo-first-order conditions (*19*), which allows substrate processing to be observed in the absence of any influence from product dissociation. In an attempt to distinguish the kinetics of base excision from those of strand cleavage, we compared the kinetics of strand cleavage by wild-type hOgg1 both with and without a piperidine quench, which chemically induces strand cleavage of the abasic intermediate (refer to Figure 1A). Briefly, a duplex 25mer ^{32}P-labeled on the oxoG-containing strand was mixed with a 30-fold molar excess of the glycosylase, and aliquots were withdrawn after certain time intervals and quenched either with buffered formamide solution or with formamide solution containing 0.5 M piperidine. The piperidine-treated samples only were heated for 5 min at 60 °C to ensure complete strand cleavage. The product mixtures were separated by denaturing PAGE, and the amount of strand-cleaved product was quantified by phosphorimage analysis. In a separate set of experiments, we determined that reaction rate is not accelerated by increasing the enzyme concentration (data not shown). Because inverse exponential kinetics were observed, we were able to derive independent pseudo-first-order rate constants (k_{obs}) for the base excision process alone and for the base excision and β-lyase reaction processes combined.

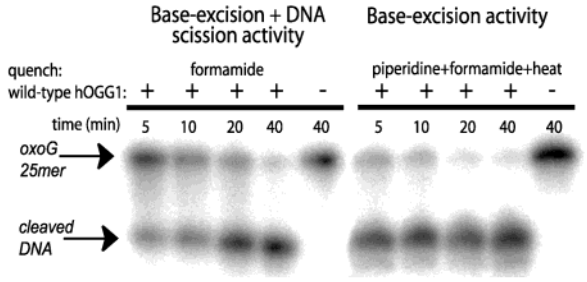

FIGURE 2: Comparison of DNA strand cleavage under enzymatic versus chemical/enzymatic conditions. The product of base excision only by hOgg1 is indistinguishable from that of the starting DNA but can be revealed by treatment with piperidine/formamide. The left-hand gel shows a time course of DNA strand cleavage by the enzyme alone, revealing the products that have undergone base excision followed by DNA strand cleavage catalyzed by the enzyme. The right-hand gel shows the sum of the products that have undergone either base excision alone or base excision plus β-lyase cleavage. Comparison of the left-hand gel with the right indicates that the product of base excision alone accumulates, indicating that strand scission is rate limiting for the wild-type enzyme under conditions in which the substrate is saturated by enzyme.

Shown in Figure 2 are the results of these cleavage experiments, which clearly demonstrate that the observed rate of base excision exceeds that of the base excision and β-lyase reactions combined. Indeed, base excision proceeded so rapidly under these conditions as to preclude precise determination of a pseudo-first-order rate constant (k_{obs}) for the base excision step, but we could estimate a lower limit of 0.34 ± 0.04 min^{-1}. This compares with a k_{obs} for the combined base excision and β-lyase reactions of 0.106 ± 0.018 min^{-1}. These results establish that base excision is faster than the β-lyase reaction, in agreement with previous experiments in which base excision was found to proceed at twice the rate of β-lyase cleavage under multiple-turnover conditions (*31*). The β-lyase chemistry is limiting overall, at least under the present conditions. On the basis of these data alone, however, we cannot distinguish whether the base excision chemistry or a conformational change preceding it determines the observed rate of base excision.

Single-Turnover Activity of the hOgg1 Mutants. The DNA strand-cleavage activities of the mutant hOgg1 proteins were compared to that of the wild-type enzyme under single-turnover conditions (*19*). In these experiments, we did not make any attempt to observe the kinetics of formation of the base-excised intermediate. Briefly, a duplex 25mer ^{32}P-labeled on the oxoG-containing strand was mixed with a 25−200-fold molar excess of the glycosylase, and aliquots were withdrawn after certain time intervals and quenched with buffered formamide solution. The product mixture was analyzed as described above. Again, the reaction rates for the mutant proteins were found to be independent of enzyme concentration (data not shown). The pseudo-first-order rate constants (k_{obs}) for these reactions are presented in Table 1.

The catalytic activity of the D268N hOgg1 mutant was found to be substantially diminished relative to that of the wild-type enzyme, with the k_{obs} being ~65-fold lower as the result of changing Asp268 to Asn (Figure 3 and Table 1). This result is consistent with those on other HhH-GPD glycosylases, having established a critical role for the active site Asp in catalysis (*8*−*11*).

Table 1: Biochemical Properties of Wild-Type and Mutant hOgg1 Proteins

	hOgg1				
	wild type	K249Q	D268N	D268E	D268Q
mp (°C)	43.0	43.0	39.5	36.0	~35
k_{obs} (min^{-1})[a]	0.106 ± 0.018		0.0016 ± 0.00027		
K_d (nM)[b]		14.0 ± 0.1	700 ± 20		

[a] Measured in single-turnover experiments using a formamide quench at 37 °C. [b] Measured on 25mer oligonucleotide containing an oxoG opposite cytosine.

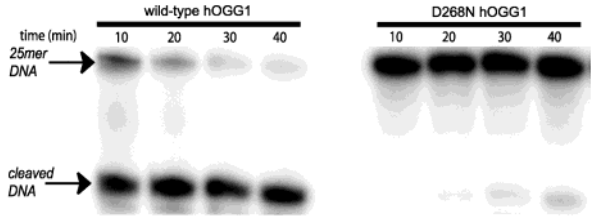

FIGURE 3: Comparison of activity of wild-type hOgg1 to D268N hOgg1. Single-turnover assays were performed with a 30-fold excess of protein over DNA. Aliquots were quenched with formamide before being loaded onto a 20% urea−PAGE gel. The D268N mutant retains residual activity but is only ~1.5% as active as its wild-type counterpart.

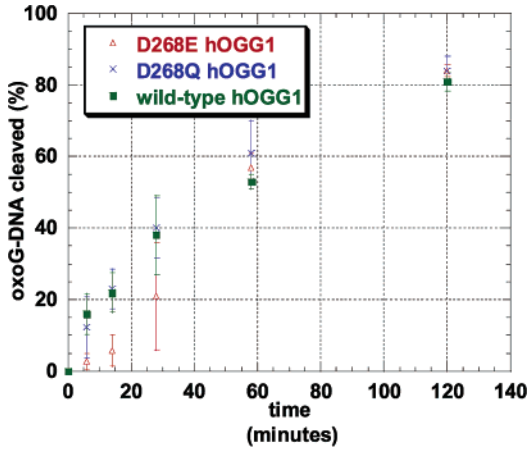

FIGURE 4: Comparison of the activities of the D268E and D268Q mutant proteins to wild-type hOgg1. Single-turnover assays were performed with a 30-fold excess of protein over DNA and were quenched with formamide. The results of triplicate runs are shown, with error bars representing the 95% confidence level for each time point. The lag phase in the D268E hOGG1 was consistently observed, though its cause is unknown.

The results of single-turnover kinetic measurements on the D268E and D268Q mutant proteins showed poor reproducibility at 37 °C. Having determined that these mutant proteins are thermally unstable at 37 °C (see below), we lowered the temperature of the cleavage assays to 25 °C. Unexpectedly, the DNA-cleavage activities determined for both mutant proteins were equivalent to that of the wild-type protein, within the uncertainty of the assay (Figure 4). For uncertain reasons, the D268E mutant consistently showed a lag in the early part of the time course.

Strand scission catalyzed by wild-type hOgg1 proceeds through an obligate Schiff base intermediate in which the ϵ-amino group of Lys249 is doubly bonded to C1′ of the ring-opened abasic site. We reasoned that it should be possible to form this intermediate independently by incubat-

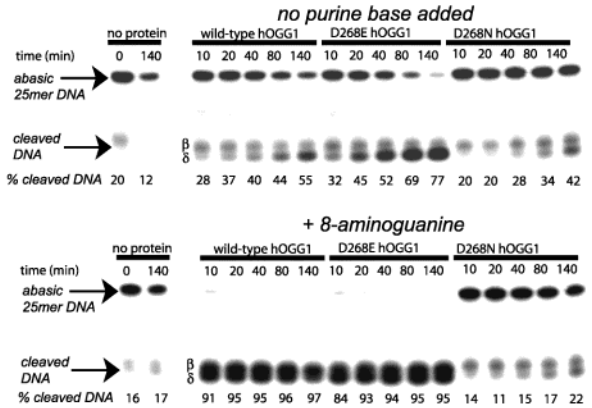

FIGURE 5: Nicking activity of wild-type hOgg1, D268E hOgg1, and D268N hOgg1 on abasic DNA. DNA containing a single abasic site was prepared from uracil containing DNA as described in the Experimental Procedures. The assay was carried out at 8 °C to avoid destabilizing D268E hOgg1, which is thermally labile. The upper panel shows strand cleavage by the enzyme in the absence of an added purine base, and the lower panel represents cleavage carried out in the presence of 50 μM 8-aminoguanine, which is known to accelerate the scission of abasic DNA (*32*). Acceleration by 8-aminoguanine is observed for both wild-type hOgg1 and D268E hOgg1 but not for D268N hOgg1.

ing the enzyme with DNA containing an abasic site. If Schiff base formation is faster than DNA strand scission, then one should be able to observe the effects of the mutations on the β-lyase reaction sequence, independent of base excision. We therefore generated a duplex 25mer containing a single, centrally located abasic site on the radiolabeled strand and incubated this with a 200-fold excess of wild-type and mutant hOgg1 proteins. The most noteworthy observations of these experiments are (i) D268E mutant hOgg1 catalyzes strand scission faster than either wild-type or D268N and (ii) the difference in the activities of wild-type versus D268N is not as great as was observed in the coupled base excision/β-lyase assays. It has been found in these laboratories that addition of certain purine analogues tremendously accelerates the rate of strand scission on abasic DNA by wild-type hOgg1 (*32*). Thus, as seen by comparison of panel b of Figure 5 with panel A, addition of 8-aminoguanine greatly accelerated the rate of DNA cleavage by wild-type hOgg1. Interestingly, the purine analogue not only failed to accelerate the rate of strand scission by the D268N mutant hOgg1 protein but perhaps even inhibited cleavage slightly.

Gel Mobility Shift Assays. Wild-type hOgg1, D268E hOgg1, and D268Q hOgg1 all process oxoG lesions on the time scale of electrophoretic mobility shift assays (EMSA), and thus their affinity for DNA containing the native lesion cannot be measured reliably. We were, however, able to carry out EMSA on the D268N mutant protein with oxoG-containing DNA, leading to the determination of an equilibrium binding constant (K_d) of 700 ± 20 nM. By way of comparison, the K249Q mutant of hOgg1, which is completely devoid of catalytic activity, binds oxoG-containing DNA with a K_d of 14.0 ± 0.1 nM (present results and ref *12*). Thus, the K249Q mutant of hOgg1 binds oxoG-containing DNA ~60-fold more tightly than the D268N mutant, corresponding to a $\Delta\Delta G$ of 2.4 kcal/mol.

Thermal Denaturation Assays. The wild-type and mutant forms of hOgg1 gave identical CD spectra at room temperature when corrected for concentration, and the shape of the curves clearly indicated that the proteins were folded (data not shown). On the other hand, the CD spectrum of wild-type hOgg1 at 70.0 °C yielded a spectrum characteristic for a denatured protein. The molar ellipticity at 222 nm is indicative of α-helical content (*20*) and therefore can be used to gauge temperature-dependent changes in protein folding. The results of the melting point analysis are summarized in Table 1. The maxima of the first-derivative plots of the temperature scans demonstrate that wild-type and K249Q hOgg1 have the same stability, each melting reproducibly at 43.0 °C. The D268N mutant of hOgg1 is less stable by 3.5 °C, and the D268E mutant is destabilized by 7.0 °C. The D268Q mutant does not appear to undergo cooperative denaturation, but we were able to estimate its melting point to be at least 8 °C less than that of the wild-type protein. These results clearly indicate that residue 268 plays an important role in stabilizing the folded structure of the enzyme, which we ascribe primarily to the helix-capping interaction between Asp268 and helix α-M.

Table 2: Crystallographic and Refinement Parameters of the Mutant hOgg1 Proteins

	D268N hOgg1−oxoG·C	D268E hOgg1−THF·C	D268Q hOgg1−THF·C
resolution (Å) (outer shell)	30−2.70 (2.87−2.70)	30−2.20 (2.34−2.20)	30−2.20 (2.34−2.20)
space group	$P6_522$	$P6_522$	$P6_522$
unit cell			
a, *b*, *c* (Å)	92.3, 92.3, 210.6	92.2, 92.2, 211.4	92.4, 92.4, 211.3
α, *β*, *γ* (deg)	90, 90, 120	90, 90, 120	90, 90, 120
completeness (%)	92.6 (90.1)	95.1 (92.4)	95.9 (92.4)
R_{merge}	13.7 (52.6)	6.1 (35.3)	6.4 (40.3)
$I/\sigma(I)$	15.0 (3.88)	22.3 (5.6)	23.0 (4.7)
total observations	88563	167899	149944
individual reflections	14671	33215	29555
R-factor	0.23 (0.31)	0.24 (0.31)	0.24 (0.33)
R_{free}	0.27 (0.37)	0.26 (0.33)	0.27 (0.34)
rmsd			
bonds (Å)	0.006	0.006	0.006
angles (deg)	1.3	1.2	1.2

Crystallographic Analysis of the Mutants. Even though the D268N mutant appeared to retain some activity (k_{obs} ~1.5% that of wild type), we were nonetheless able to grow crystals of the mutant enzyme complexed with oxoG-containing DNA. It is possible that the residual activity of the mutant protein is suppressed in the buffer solution used for crystallization. To prepare crystals of the D268E and D268Q mutant proteins, which retain base excision and β-lyase activity, we crystallized these variants in complex with DNA containing a noncleavable abasic site analogue, the tetrahydrofuranyl abasic site (THF). Diffraction data for the crystals were collected using a synchrotron source, and the structures were solved by molecular replacement. All three crystal forms belong to the same space group and have the same unit cell parameters as K249Q hOgg1 in complex with oxoG DNA (*12*). The crystallographic data are summarized in Table 2.

Overall, the structures of the mutant proteins complexed with DNA are very similar to each other and to that of the K249Q complex (*12*). The root mean square deviation (rmsd) of the protein backbone between the D268N and K249Q hOgg1 structures (*13*) is 0.32 Å. The backbone rmsd

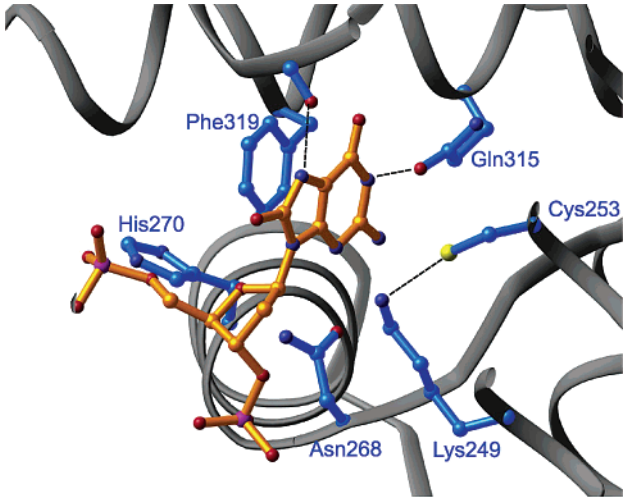

FIGURE 6: Active site structure of D268N hOgg1 complexed with oxoG-containing DNA. This is the first structure of a glycosylase/β-lyase containing its intact active site nucleophile in the presence of lesion-containing DNA. Lys249 is ordered, but it is not well positioned for in-line attack to displace the oxoG base. Asn268 is N-capping helix α-M, the long axis of which runs perpendicular to the page. Unlike Asp268, Asn268 is not involved in a hydrogen bond interaction with His270.

comparing the structures of wild-type versus D268E hOgg1 bound to the THF analogue is 0.45 Å and is 0.59 Å for the wild type/THF versus D268Q hOgg1/THF, demonstrating that no global structural change is brought about by the amino acid changes. In all three structures, the only significant differences are concentrated in the active site region, particularly in the first three residues of helix α-M (residues 269, 270, and 271). In each of the three structures, the nucleophilic ϵ-NH_2 of Lys249 has a *B*-factor that is 13% lower than the average of the other Lys residues in each structure. This indicates that the ϵ-NH_2 group adopts a relatively fixed position in the crystal, even though it lies at the end of a long alkyl chain.

The D268N hOgg1 structure is the first to contain the cognate base in the presence of the active site nucleophile. In this structure, the ϵ-NH_2 group of Lys249 is positioned near C1′ (3.4 Å) but is not in a suitable trajectory for in-line nucleophilic attack on the glycosidic bond (Figure 6). More intriguingly, the ϵ-NH_2 of Lys249 appears to be hydrogen bonded to the sulfhydryl of Cys253, which in turn is in van der Waals contact with the π-face of the oxoG nucleobase. Because Cys253 is positioned on the top face of the sugar, it is impossible for Lys249 to maintain its contact with Cys253 while attacking the sugar from the under side. As with the wild-type enzyme, the carbonyl of Asn268 caps the N-terminus of helix α-M by hydrogen bonding to the main chain amide of Met271. Whereas the other carboxyl oxygen of Asp268 in the wild-type enzyme is hydrogen bonded to the side chain of His270, the side chain amide $-NH_2$ of Asn268 in the D268N mutant protein is too far removed from His270 for hydrogen bonding to take place; the loss of this interaction may help to explain the relatively weak binding of the D268N mutant protein to DNA, because His270 interacts directly with the DNA phosphate backbone on the 5′-side of the lesion. The rest of the active site and base recognition pocket, including the recognition of oxoG, is essentially identical in the structures of D268N and K249Q hOgg1 (*12*) bound to oxoG-containing DNA.

The structure of D268E hOgg1 complexed with the THF inhibitor reveals that Glu268 maintains a helix-capping interaction with the backbone amide of Met271. However, to establish this interaction, the residue is forced to adopt a highly dispreferred conformation (Figure 7C), because it causes the Cα−Cβ and Cδ═O bonds to become engaged in the sterically repulsive *syn*-pentane interaction. The other carboxylate oxygen of Glu268 appears to hydrogen bond with the imidazole ring of His270, similar to the wild-type enzyme. The carboxylate group of Glu268 is 6.4 Å from the ϵ-NH_2 group of Lys249, a separation that would require side chain reorganization for the two to participate in general acid/base chemistry.

The structure of D268Q hOgg1 in complex with the THF inhibitor shows significant differences in the active site from that of D268E hOgg1 (Figure 7B). The side chain of the Gln268 is involved in a conformationally strained capping interaction with the main chain amide of Met271, although the geometry of the capping hydrogen bond is less optimal than with Glu268, owing to 50° rotation of the Cγ−Cδ bond relative to its orientation in the D268E structure. This rotation moves the side chain amide out of range of His270, and it allows a water molecule to insert itself into the structure, simultaneously hydrogen bonding to the Gln268 side chain amide and the ϵ-NH_2 of Lys249 (Figure 7). Intriguingly, this water is well positioned for attack on C1′ of the substrate.

DISCUSSION

Helix Capping by Asp268 Stabilizes the Folded Structure of hOgg1. Despite the high conservation of folded structure among members of the HhH-GPD superfamily of DNA glycosylases, the amino acid sequences of these enzymes vary widely. Indeed, only one residue is absolutely conserved in these enzymes, the aspartate that defines the C-terminal end of the HhH-GPD motif (Asp268 in hOgg1). Here we have examined the role of this residue through biochemical and biophysical studies.

In all structures of HhH-GPD glycosylases determined to date (*9*, *10*, *12*−*15*, *21*−*23*), the active site Asp is observed to act as an N-terminal helix "cap" for an α-helix (α-M in hOgg1) that forms an integral component of the enzyme active site. This particular type of intramolecular interaction, first noted by Kendrew in the structure of sperm whale myoglobin (*24*), entails an amino acid side chain at the N-terminal end of an α-helix reaching forward to hydrogen bond with one or more main chain amide protons in the first turn of the helix (refer to Figure 1C) (*25*). This side chain hydrogen bond thus substitutes for the main chain/main chain hydrogen bonds that would be formed in an elongated helix. There exist distinct preferences for N-cap residues, with Asp, Asn, Ser, and Thr being the most highly preferred. Interestingly, although Glu and Gln possess hydrogen-bonding functionality in their side chains, these residues are rarely employed as helix N-caps (*25*), suggesting some deficiency in their ability to serve in this function. The present structural results on the D268E and D268Q mutants of hOgg1 suggest a clear reason why these two residues have poor capping ability: the side chain conformation required to establish an N-cap hydrogen bond can be achieved only at the expense of a severe steric clash known as a *syn*-pentane interaction (*26*). Despite this steric clash, the Glu and Gln mutant

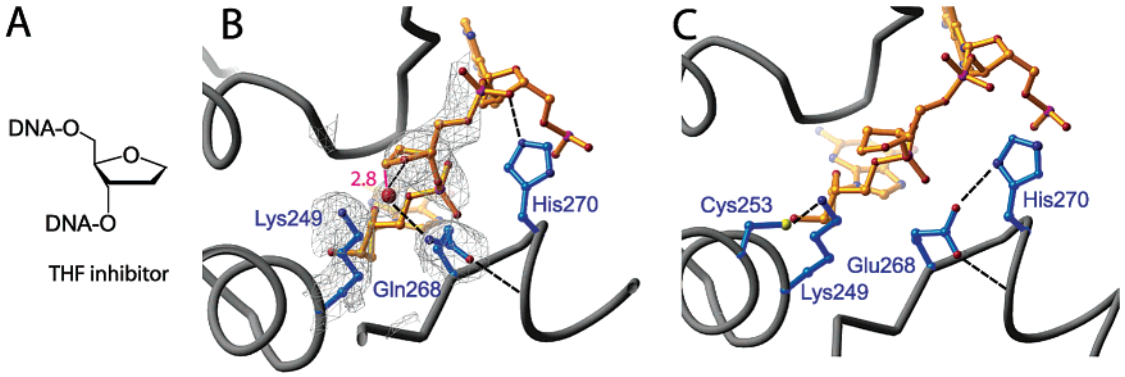

FIGURE 7: (A) Chemical structure of the THF inhibitor that was used in the crystallization of D268E and D268Q hOgg1. (B) Active site structure of D268Q hOgg1. Key active site residues are shown, along with hydrogen-bonding interactions (black dashes). The experimental electron density is shown to demonstrate the presence of the water molecule between Gln268 and the deoxyribose ring. The distance between the observed water molecule and C1′ of the deoxyribose moiety is shown (Å, magenta line). The sterically unfavorable *syn*-pentane conformation of Gln268 can be observed. (C) Active site of D268E. Note the *syn*-pentane conformation adopted by the side chain of Glu268.

proteins still exhibit N-capping at position 268, perhaps because the capping interaction is enforced upon association with DNA.

The present data on thermal denaturation of the wild-type and mutant hOgg1 proteins clearly demonstrate the importance of the Asp268 N-cap interaction for stabilizing the protein fold and yield a rank order for the relative strength of the capping interaction among the variants studied here. Consistent with the foregoing discussion, mutation of Asp268 to Glu or Gln has a seriously deleterious effect on the thermal stability of hOgg1; in fact, the D268Q mutant protein did not even show cleanly cooperative melting behavior and was prone to denaturation during purification. Mutation of Asp268 to Asn also decreased the melting temperature of the protein, but by a more modest amount (3.5 °C). This effect may be due to the weaker hydrogen-bonding capability of a neutral versus a negatively charged acceptor (*27*) and to the loss of a favorable electrostatic interaction between the negatively charged Asp side chain and the positive dipole at the N-terminal end of the α-helix (*28*).

Whereas mutations at position 268 affected the protein stability, changing Lys249 to Gln had no effect. It is tempting to speculate that the lack of an effect upon altering a formally charged residue (Lys) to a neutral one (Gln) may suggest that the pK_a of Lys249 is anomalously low.

Function of Residue 268 in Catalysis of Base Exicision. The hOgg1 enzyme catalyzes two sequential biochemical transformations, base excision and then β-lyase strand cleavage, both of which may involve multiple elementary reaction steps (Figure 1A). Although the principal residues required for catalysis of base excision, Lys249 and Asp268, have been known for years, the role of Asp268 in catalyzing this transformation has remained unclear. An obvious possibility is that Asp268 assists base excision by deprotonating Lys249, thereby converting it from the unreactive cationic form to the nucleophilic neutral amine. Arguing against this scenario is the fact that an Asp residue acting as a helix cap should be less basic than a typical Asp by several orders of magnitude, and this stable interaction would have to be completely disrupted for Asp268 to rotate around and reach Lys249. The one cocrystal structure that is available of the wild-type protein, bound to an abasic substrate analogue (*13*), shows no interaction between Asp268 and Lys249. Indeed, the only structure in which these two residues are hydrogen bonded is that of the free protein, in which Asp268 preserves its capping interaction and Lys249 swivels about to contact it. Significantly, even with the weakened capping interaction and elongated side chain of the D268E mutant protein, the Glu side chain still does not interact with Lys249. The possibility that these ground state structures do not reveal a high-energy conformer of Asp268 that abstracts a proton from Lys249 cannot be excluded, but there is not necessarily any need to invoke such a scenario. If the pK_a of Lys249 is lowered even modestly by the local microenvironment of the enzyme active site, enough of the neutral amine should be present to allow base excision to proceed.

An alternative possibility is that Asp268 electrostatically stabilizes the developing positive charge on $O^{4'}$ in the transition state of the base excision step (*13*). Consistent with this notion, in all of the hOgg1 cocrystal structures having an Asp at position 268, the carboxylate oxygen is positioned nearest $O^{4'}$, with the two separated in some cases by as little as 3.2 Å. Owing to the capping interaction, the orientation of the Asn268 side chain is nearly identical to that of Asp268; hence substitution of Asn at position 268 essentially replaces a partially anionic oxygen atom for a neutral NH_2 group at the same location within the active site. The distance between the side chain amide nitrogen of Asn268 and $O^{4'}$ of the deoxyribose ring is longer (3.4 Å) than would be expected for hydrogen bonding between the two (*29*) but is close enough that $O^{4'}$ would experience the partially positive electrostatic field of the amide protons on Asn268. We thus favor the explanation that the charge reversal in going from Asp (δ^-) to Asn (δ^+) at position 268 raises the transition state energy for base excision by destabilizing the developing positive charge at $O^{4'}$, thereby leading to a dramatic reduction in the rate of base excision.

The D268N structure is the first structure of hOgg1 available with both the catalytic Lys and an intact oxoG lesion base. The positioning of Lys249 in this structure is interesting, being close to C1′ but not on a trajectory that is compatible with in-line displacement to expel the base by an S_N2-like mechanism (Figure 8A). Also noteworthy is that fact that the ϵ-nitrogen atom of Lys249 is within hydrogen-bonding distance of Cys253, which in turn is in van der Waals contact with the oxoG base. Calculations recently performed on uracil−DNA glycosylase indicate that this monofunctional glycosylase employs a dissociative (S_N1-like)

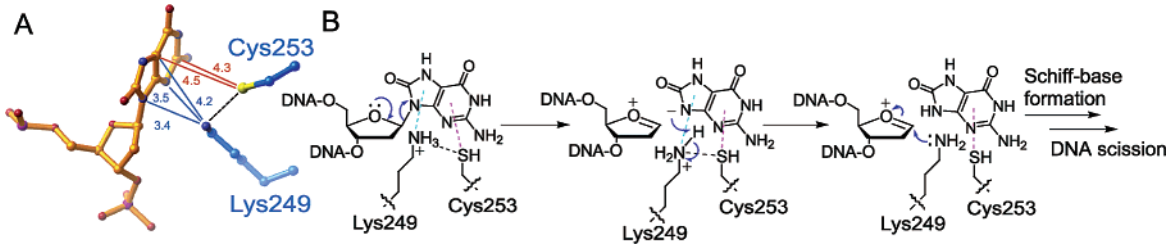

FIGURE 8: (A) Relation of Lys249 and Cys253 to the oxoG base in the D268N hOgg1 structure. Distances shown are in angstroms. The black dashed line between Lys249 and Cys253 represents a hydrogen bond. Note the positioning of Lys249, which is inconsistent with its direct displacement of the oxoG base. (B) Putative dissociative mechanism of hOgg1 base excision. The light blue dashed line between Lys249 and the face of oxoG represents a potential cation−π interaction. The purple dashed line between Cys253 and the face of oxoG represents a van der Waals contact. The black dashed line represents the observed hydrogen bond between Lys249 and Cys253. In this mechanism, dissociation of the anionic oxoG base, which would be stabilized by its interaction with the cationic nitrogen atom of Lys249, is followed by transfer of a proton from Lys249 to oxoG. The resultant neutral amine on Lys249 would then capture the oxocarbenium intermediate of the deoxyribose moiety. Subsequent Schiff base formation would be followed by DNA strand cleavage.

mechanism (*30*), suggesting that the possibility should at least be considered that hOgg1 likewise employs a dissociative mechanism. Any interaction that would stabilize the incipient negative charge on the oxoG during rupture of the glycosidic bond would facilitate base excision by a dissociative mechanism. In this regard, we note that the positioning of Lys249 in the D268N structure suggests a cation−π interaction between the ammonium form of Lys249 and the oxoG base could readily be accommodated (Figure 8A); this type of interaction would make a favorable contribution to dissociative base excision. Lys249 would then have to be deprotonated, perhaps by the oxoG anion (*32*; note that this mechanism might not pertain equally to excision of a FaPy lesion by hOgg1), in order for it to form a bond with the sugar oxocarbenium ion intermediate (Figure 8B). One interesting consequence of invoking a dissociative mechanism is that it does not require nucleophilic substitution at C1′ to proceed with inversion of stereochemical configuration; indeed, the D268N structure suggests that retention may be more likely. The stereochemistry of nucleophilic substitution by hOgg1 is presently unknown.

Function of Asp268 in DNA Strand Cleavage. While the function of Lys249 in β-lyase activity can be inferred unambiguously on chemical grounds, the participation of Asp268 in this transformation is less obvious. Here we have examined this issue by forming the key Schiff base intermediate in the β-lyase transformation by a process that avoids hOgg1-catalyzed base excision. In the absence of an added purine base, the D268N mutant of hOgg1 catalyzes base excision with only a modest reduction in rate relative to the wild-type protein. However, under the more physiologic conditions in which a purine base is present, and substrate processing by the wild-type protein is dramatically accelerated, D268N hOgg1 is nearly devoid of β-lyase activity. This loss of activity could be due to the Asn amide group hydrogen bonding to functional groups involved in the β-lyase cascade, for example, the purine base, in such a way as to interfere with obligate proton-transfer operations. Significantly, the D268E mutant hOgg1 is effective at promoting DNA strand scission. The D268Q mutant was not analyzed in these experiments. These results provide suggestive evidence that a carboxylate-bearing residue at position 268 promotes DNA strand scission. We have proposed that the purine base is responsible for most, if not all, of the proton-transfer steps in the β-lyase cascade (*32*); if this holds true, then Asp may be involved in orienting the substrate sugar moiety in a conformation that allows chemistry to take place.

Catalytic Mechanism of the Glu268 and Gln268 Mutants. The present observation that the D268E and especially the D268Q mutant hOgg1 proteins are catalytically active was completely unexpected, considering the absolute conservation of Asp268 and the strained conformation of the 268 side chain in the DNA complexes of these proteins. It seems likely that the D268E mutant protein uses a mechanism similar to that of the wild-type protein, with the carboxylate stabilizing the incipient oxocarbenium ion intermediate and perhaps helping to orient the substrate during the β-lyase cascade.

The activity of the Gln268 mutant is perplexing, especially in light of the fact that the D268N protein is so catalytically ineffective. The structure of this mutant bound to the THF abasic site analogue raises the intriguing possibility that the D268Q protein actually uses a different mechanism from that employed by the wild-type protein. Significantly, the structure reveals the presence of an ordered water molecule wedged between Lys249 and the amide $-NH_2$ of Gln268 (Figure 7B). These interactions not only position the water directly underneath C1′ but could also assist in the stabilization of a nucleophilic hydroxide ion. Thus, the structure raises the intriguing possibility that the D268Q mutation endows hOgg1 with the ability to perform base excision by a mechanism like that of monofunctional glycosylases; the abasic site thus generated would be captured subsequently by Lys249, and the β-lyase cascade would ensue. Adding further to the mystery is the fact that the D268Q mutant protein is so proficient at catalyzing DNA strand scission, when the D268N mutant is so ineffective.

ACKNOWLEDGMENT

The authors thank J. C. Fromme for sharing unpublished results and for discussion regarding the 8-aminoguanine assay.

SUPPORTING INFORMATION AVAILABLE

Melting curves of the wild-type, K249Q, D268N, D268E, and D268Q forms of hOgg1. This material is available free of charge via the Internet at http://pubs.acs.org.

REFERENCES

1. Michaels, M. L., and Miller, J. H. (1992) The GO system protects organisms from the mutagenic effect of the spontaneous lesion 8-hydroxyguanine (7,8-dihydro-8-oxoguanine), *J. Bacteriol. 174*, 6321−6325.

2. Grollman, A. P., and Moriya, M. (1993) Mutagenesis by 8-oxoguanine: an enemy within, *Trends Genet. 9*, 246−249.
3. Hainaut, P., Hernandez, T., Robinson, A., Rodriguez-Tome, P., Flores, T., Hollstein, M., Harris, C. C., and Montesano, R. (1998) IARC Database of p53 gene mutations in human tumors and cell lines: updated compilation, revised formats and new visualisation tools, *Nucleic Acids Res. 26*, 205−213.
4. Friedberg, E. C., Walker, G. C., and Siede, W. (1995) *DNA Repair and Mutagenesis*, ASM, Washington, DC.
5. Scharer, O. D., and Jiricny, J. (2001) Recent progress in the biology, chemistry and structural biology of DNA glycosylases, *Bioessays 23*, 270−281.
6. Hollis, T., Lau, A., and Ellenberger, T. (2001) Crystallizing thoughts about DNA base excision repair, *Prog. Nucleic Acid Res. Mol. Biol. 68*, 305−314.
7. McCullough, A. K., Dodson, M. L., and Lloyd, R. S. (1999) Initiation of base excision repair: glycosylase mechanisms and structures, *Annu. Rev. Biochem. 68*, 255−285.
8. Nash, H. M., Bruner, S. D., Scharer, O. D., Kawate, T., Addona, T. A., Spooner, E., Lane, W. S., and Verdine, G. L. (1996) Cloning of a yeast 8-oxoguanine DNA glycosylase reveals the existence of a base-excision DNA-repair protein superfamily, *Curr. Biol. 6*, 968−980.
9. Labahn, J., Scharer, O. D., Long, A., Ezaz-Nikpay, K., Verdine, G. L., and Ellenberger, T. E. (1996) Structural basis for the excision repair of alkylation-damaged DNA, *Cell 86*, 321−329.
10. Thayer, M. M., Ahern, H., Xing, D., Cunningham, R. P., and Tainer, J. A. (1995) Novel DNA binding motifs in the DNA repair enzyme endonuclease III crystal structure, *EMBO J. 14*, 4108−4120.
11. Wright, P. M., Yu, J., Cillo, J., and Lu, A. L. (1999) The active site of the *Escherichia coli* MutY DNA adenine glycosylase, *J. Biol. Chem. 274*, 29011−29018.
12. Bruner, S. D., Norman, D. P., and Verdine, G. L. (2000) Structural basis for recognition and repair of the endogenous mutagen 8-oxoguanine in DNA, *Nature 403*, 859−866.
13. Norman, D. P., Bruner, S. D., and Verdine, G. L. (2001) Coupling of substrate recognition and catalysis by a human base-excision DNA repair protein, *J. Am. Chem. Soc. 123*, 359−360.
14. Kuo, C. F., McRee, D. E., Fisher, C. L., O'Handley, S. F., Cunningham, R. P., and Tainer, J. A. (1992) Atomic structure of the DNA repair [4Fe-4S] enzyme endonuclease III, *Science 258*, 434−440.
15. Guan, Y., Manuel, R. C., Arvai, A. S., Parikh, S. S., Mol, C. D., Miller, J. H., Lloyd, S., and Tainer, J. A. (1998) MutY catalytic core, mutant and bound adenine structures define specificity for DNA repair enzyme superfamily, *Nat. Struct. Biol. 5*, 1058−1064.
16. Sarkar, G., and Sommer, S. S. (1990) The "megaprimer" method of site-directed mutagenesis, *BioTechniques 8*, 404−407.
17. Otwinowski, Z. M. W. (1996) Processing of X-ray diffraction datacollected in oscillation mode, *Methods Enzymol. 276*, 307−326.
18. Brunger, A. T., Adams, P. D., Clore, G. M., DeLano, W. L., Gros, P., Grosse-Kunstleve, R. W., Jiang, J. S., Kuszewski, J., Nilges, M., Pannu, N. S., Read, R. J., Rice, L. M., Simonson, T., and Warren, G. L. (1998) Crystallography & NMR system: A new software suite for macromolecular structure determination, *Acta Crystallogr., Sect. D: Biol. Crystallogr. 54*, 905−921.
19. Porello, S. L., Leyes, A. E., and David, S. S. (1998) Single-turnover and pre-steady-state kinetics of the reaction of the adenine glycosylase MutY with mismatch-containing DNA substrates, *Biochemistry 37*, 14756−14764.
20. Chen, Y. H., Yang, J. T., and Martinez, H. M. (1972) Determination of the secondary structures of proteins by circular dichroism and optical rotatory dispersion, *Biochemistry 11*, 4120−4131.
21. Hollis, T., Ichikawa, Y., and Ellenberger, T. (2000) DNA bending and a flip-out mechanism for base excision by the helix-hairpin-helix DNA glycosylase, *Escherichia coli* AlkA, *EMBO J. 19*, 758−766.
22. Teale, M., Symersky, J., and DeLucas, L. (2002) 3-Methyladenine-DNA glycosylase II: The crystal structure of an AlkA-hypoxanthine complex suggests the possibility of product inhibition, *Bioconjugate Chem. 13*, 403−407.
23. Bjoras, M., Seeberg, E., Luna, L., Pearl, L. H., and Barrett, T. E. (2002) Reciprocal "flipping" underlies substrate recognition and catalytic activation by the human 8-oxo-guanine DNA glycosylase, *J. Mol. Biol. 317*, 171−177.
24. Kendrew, J. C., Watson, H. C., and Strandberg, B. E. D. R. E. (1961) A partial determination by X-ray methods, and its correlation with chemical data, *Nature 190*, 666.
25. Richardson, J. S., and Richardson, D. C. (1988) Amino acid preferences for specific locations at the ends of alpha helices, *Science 240*, 1648−1652.
26. Dunbrack, R. L., Jr., and Karplus, M. (1994) Conformational analysis of the backbone-dependent rotamer preferences of protein side chains, *Nat. Struct. Biol. 1*, 334−340.
27. Saenger, W., and Jeffrey, G. A. (1991) *Hydrogen Bonding in Biological Structures*, Springer-Verlag, Berlin.
28. Serrano, L., and Fersht, A. R. (1989) Capping and alpha-helix stability, *Nature 342*, 296−299.
29. Schulz, G. E. (1979) *Principles of Protein Structure*, Springer-Verlag, New York.
30. Dinner, A. R., Blackburn, G. M., and Karplus, M. (2001) Uracil-DNA glycosylase acts by substrate autocatalysis, *Nature 413*, 752−755.
31. Hill, J. W., Hazra, T. K., Izumi, T., and Mitra, S. (2001) Stimulation of human 8-oxoguanine-DNA glycosylase by AP-endonuclease: potential coordination of the initial steps in base excision repair, *Nucleic Acids Res. 29*, 430−438.
32. Fromme, J. C., Bruner, S. D., Yang, W., Karplus, M., and Verdine, G. L. (2003) Product-assisted catalysis in base-excision DNA repair, *Nat. Struct. Biol.* (in press).

BI026823D